CrossMark

ORIGINAL PAPER

Refined simulation of temperature distribution in molds during autoclave process

Fei Chen[1] · Lihua Zhan[1] · Shujian Li[1]

Abstract Since the production of advanced composites, they have gained popularity in many industrial applications because of their unique performances. The advantages of these materials are very important, especially in the area of aviation. Among all the molding methods adopted in their production, the autoclave stands out as distinct method. Considering the temperature distribution in molds, it is one of the crucial aspects to impart quality to composite components during the process of autoclave molding, and it is necessary to do research and analysis on temperature distribution in molds, especially those of large frame-type molds. In previous studies, many authors improved the simulation accuracy simply by changing the grids or boundary conditions. A few of them took boundary layer grids into consideration for further precision. With the aid of computer softwares, this paper conducts simulation on large frame type of molds. Given that the boundary layer grids will largely determine the simulation precision, this study attempts to give emphasis on the study of boundary layer grids to make the simulation results more accurate, and finally make a comparison with the experimental data. The error between simulation and experiment results was within 5 %. This indicated that the boundary layer grids had great influence on the accuracy of simulation of the paper conducted, and should be given more attention. Therefore, the method of simulation in this study can be further used to accurately simulate the temperature distribution in molds.

Introduction

Advanced composites have been widely applied in aviation due to their excellent performances, such as high-specific strength and stiffness, good weight loss of structure, the improvement of aircraft performance, and so on. As known, the quantity of composite components in aircraft has become a crucial sign to measure the advanced performance of aircraft design [1, 2]. The autoclave process can better make advanced composites to achieve the key performances mentioned above, especially for large composite components. In manufacturing process of large composite components, large molds are often employed to assist their forming process. It may be a reason for large frame type molds to become so popular. As for the forming quality of large components, the temperature uniformity at the mold surface is an influential factor, which plays important role of "wind indicator" during autoclave process. Many factors influence the temperature distribution of large frame type molds, such as the heat exchange of gas within autoclave, the structure of molds, the heat-transfer characteristic of craftwork accessories attached at the mold surface, and the complicated structure of molds themselves. Therefore, it is difficult to exactly predict the molds' temperature distribution [3]. It is a valid way to adopt experimental methods independently to obtain the temperature distribution, but it is time-consuming and costly. Therefore, at present, computer simulation technology has become a popular way to obtain the approximate temperature distribution in molds, because of the high efficiency and low cost, and the issues of simulation on temperature distribution can be solved well.

✉ Lihua Zhan
  yjs-cast@csu.edu.cn

1   Light Alloy Research Institute of CSU, Central South
     University, Changsha 410083, China

IPPI   Springer

Many relevant studies have been carried out by focusing on composite materials, molds, and temperature distribution of mold formation. Nakhaei et al. [4] studied the composites as they had widely applied to automotive and aerospace fields, and studied some parameters that may influence the composites. Gniatczyk et al. [5] discussed that the thermal conductivity of molds could be raised through an "egg box" of metal frame structure, and pointed out that selection of spacing was decided by different materials in the process of design. Michael et al. [6] illustrated the advantages of molds of frame-type structure, and thought that these molds could not only reduce weight, but also could accelerate the heat transfer. Prasad et al. [7] attempted to combine the banana fiber with low-density polyethylene to produce composite materials that would be environmental and friendly. In their study, they also discussed the effect of banana fiber surface treatment and compatibilizer addition to composite materials. Bahramian et al. [8] illustrated some information about the effect of the external heat flux through calculating the effective thermal diffusivity and doing evaluation on ablation performances. Duval studied the heat-transfer mechanism of molds fabricated by carbon fiber/epoxy composite materials, and carried simulation on the three-dimensional transient temperature distribution of the molds. Finally, he made a comparison of both experimental and simulation results to prove the reliability of simulation data [9]. Hudek studied the effects of various factors on heat-transfer coefficient, and their research results showed that the probable influential factors were as follows: vacuum bags, the status of composite components in autoclaves, the disposition of molds, heat flow direction of the open air and etc. At the end of his research, the heat-transfer coefficient was successfully modeled [10]. Pirouzfar et al. [11] studied the design and optimization of carbon–carbon composites to investigate the influence of each parameter. Through the modification of parameters, they finally concluded that heat shields provided more heat resistance than the composites derived from resole. Ding et al. [12] studied composites of functional graphene nanoflakes/cyanate/epoxy and by making comparison they concluded that functional graphene nanoflakes could be used as catalyst and shorten curing time. Vafayan et al. [13] presented the better thermal cure cycle with the aid of softwares: Abaqus and Matlab, because an optimized thermal cure cycle could ensure the curing uniformity of complex-shape composite parts. Gao et al. simulated the temperature rising process in autoclave through numerical computation method. In their studies, the distribution of the fluid field and temperature field in autoclave were obtained, and the accuracy of simulation results was verified by comparing with the experimental data [14]. Zhang et al. [15] simulated three different air flues of straight-shape, cross-shape, and T-shape with the help of FLUENT software, and the results showed that the T-shaped air flue is the optimal choice compared with other two shapes. Yue et al. [16] studied the effect of mold on deformation of composite components. The results indicated that composite components can generate residual stress imposed by the mold limitations, which further lead to the deformation of composite components. The significance of mold temperature distribution was also demonstrated. Zhang investigated the influence of technological and environmental parameters on temperature distribution in mold, and further simplified the simulation model [17].

Among many attempts, the most common method used in simulation has been the K-e turbulence model. Some researchers have studied the rules of simulation under certain parameters, but do not indicate on how to enhance the accuracy of simulation. Some studies have just verified the precision of simulation by specific parameter settings. However, the actual situations in the autoclave process is rather complex, and the K-e turbulence model cannot simulate the temperature distribution accurately. In this study, the simulation model has been established on the basis of Ref. [14]. As a more appropriate model for the mold frame, the SST model is employed to study the temperature distribution further. In addition, the study of boundary layer at the interface between the fluid and solid is rather few, but it is undeniable that the boundary layer is a key point to conjugate heat transfer in simulation process, and cannot be ignored. As a result, the boundary layer analysis has been added in this study to ensure higher accuracy. Therefore, the two aspects discussed above are considered to perform a specific simulation. The results of simulation and experimental data from the 14th literature citation are compared carefully, and the simulation results are verified at the end.

Experimental

The autoclave model

As shown in Fig. 1, an autoclave mainly includes the following parts: fan, heating equipment, pressure vessel, gas pressure device, corresponding control system, and vacuum system. There is a slide passage and object stage in the pressure vessel. The object stage is set up to support the mold. As the main part of the autoclave, pressure vessel can be realized by means of modeling. Other parts of the autoclave can be achieved through setting the corresponding boundary conditions in the simulation.

The working principles of autoclave

To establish the valid autoclave model, the structure and working principles of autoclave should be introduced in

Fig. 1 Autoclave model
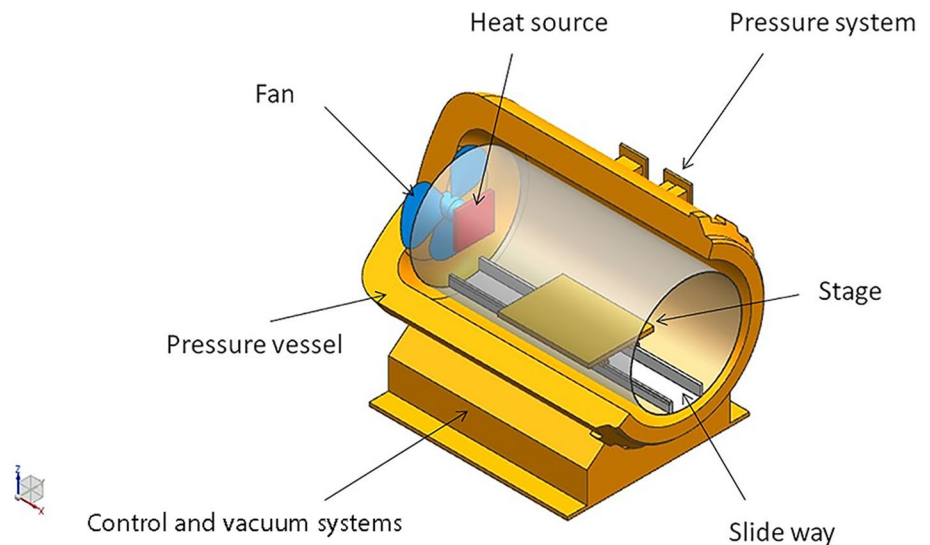
Fig. 2 The diagram of autoclave structure
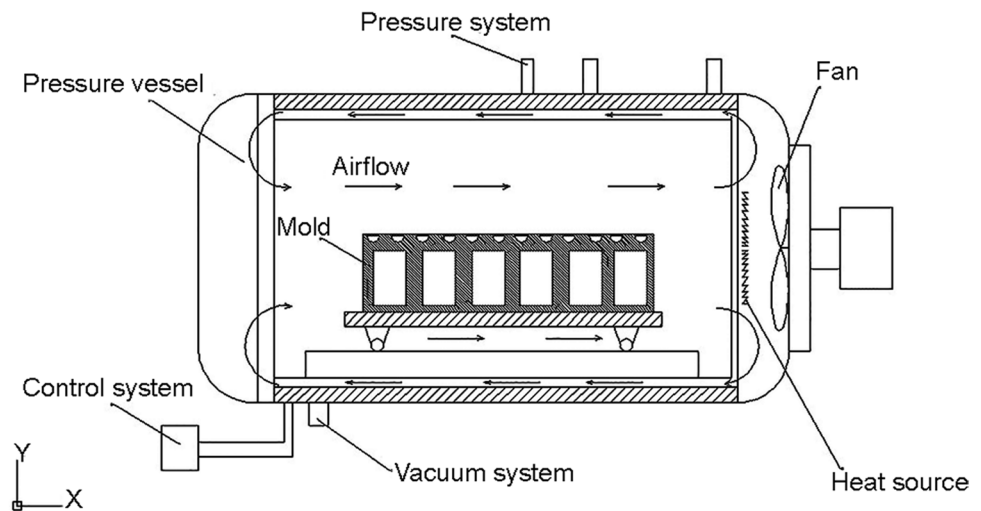
detail. The autoclave structure is shown in Fig. 2. During the autoclave process, the electric hot wire is the heat source, the fluid is chosen to be the heat-transfer medium (it is usually air), and the fan is used as the motive power to force gas cycle [18]. After the specific settings, the electric hot wire is employed to heat the mold component.

Heat-transfer pattern

Heat conduction, heat convection, and thermal radiation are three ways of heat transfer. Among them, the way of thermal radiation may be taken in consideration only at a higher temperature. As the temperature of autoclave is less than 180 °C during the formation process, the thermal radiation passage can be ignored. Temperature changes of mold frame structure in autoclave are mainly due to the forced heat convection between the mold and high-temperature gas, and the occurrence of heat conduction in the mold,

as shown in Fig. 3. Therefore, the simulation of temperature distribution for mold component by autoclave process only considers two passages of heat convection and heat conduction.

In addition to the above elaborations, other contents are needed to be added as follows: the fluid by its nature is usually a kind of viscous fluid. When the viscous fluid flows through the solid walls, due to the stickiness of fluid, the flow velocity will gradually decelerate as the fluid becomes closer to the walls, and the fluid will be stopped and kept in non-slipping state and adherence position to walls, as shown in Fig. 4. In the adherence position to walls, the thin layer of fluid is relatively static compared with the walls. The heat transfer between the thin layer of fluid and walls is in terms of passage of heat conduction. Therefore, the thin layer of fluid directly decides the accuracy of the simulation. In hydromechanics, this thin layer of fluid is named the "boundary layer".

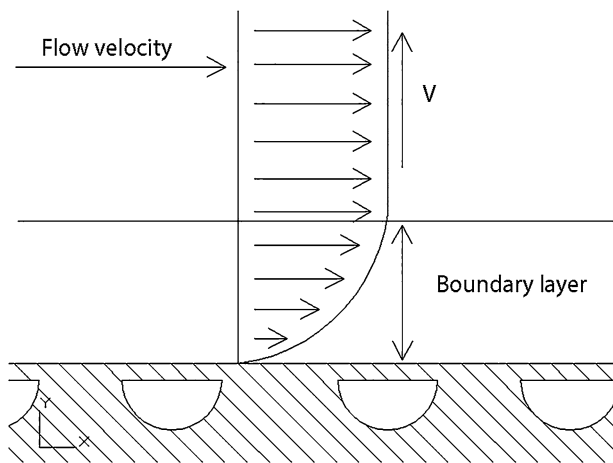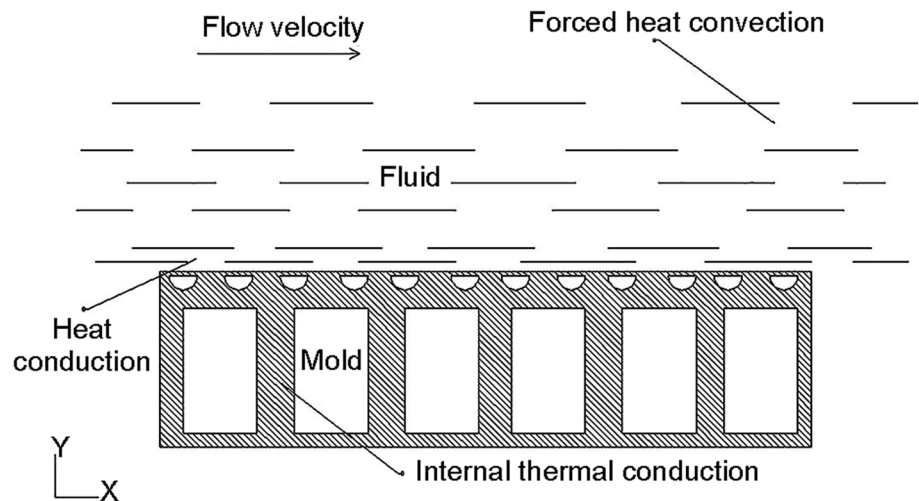**Fig. 3** Heat-transfer pattern in autoclave

Fig. 4 The velocity variation closed to the wall

Fig. 5 Typical frame type mold for autoclave

The mold model and material

The study in this paper is based on large frame-type molds, widely used in the manufacturing industry of aerial composite materials. As Fig. 5 shows, the mold is made up of four parts: equalizing hole, aspirail, panel, and some support grids [19]. The thickness of molds' top surface is 7 mm. All the grids' thicknesses are 4 mm. Radius of every equalizing hole is 25 mm, and the approximate dimension of aspirail is 130 mm × 220 mm. The mold material is steel and its whole size is 1700 mm × 1500 mm × 400 mm (length × width × height). The support grids play the role of supporting and maintaining the stiffness. The equalizing hole and aspirail are designed to make the airflow and the solid perform heat convection better.
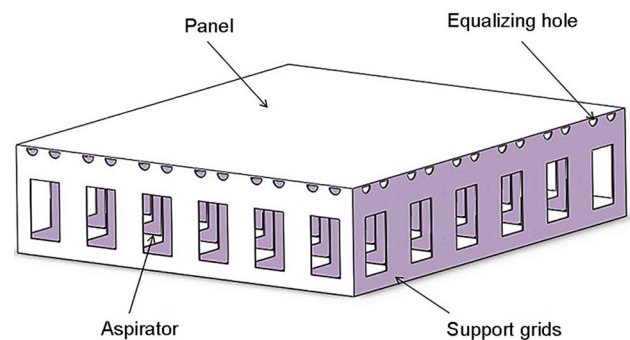
Analysis of gas flow condition

The heat-transfer route of autoclave process is shown in Fig. 6. Generally, there are two heat sources in the autoclave, heating devices (electric heat source) and the released heat generated from the curing reaction of composite components (internal heat source). Due to the limited influence of the released heat on mold component, the released heat is not needed to be considered. In addition, the heat generated from curing reaction may be transferred from mold to air through the heating devices.

In general, the heating process of mold in autoclave is realized through forced convective heat transfer of fluid. Therefore, the flow state of fluid must be considered in simulation. The flow of fluid can be divided into laminar flow and turbulent flow. In autoclave, the flow belongs to internal flow. For further evaluation, it belongs to laminar flow or turbulent flow, and the Reynolds number (Re) is always used to produce results. The Re is defined as:

Fig. 6 Heat-transfer route of formation technology
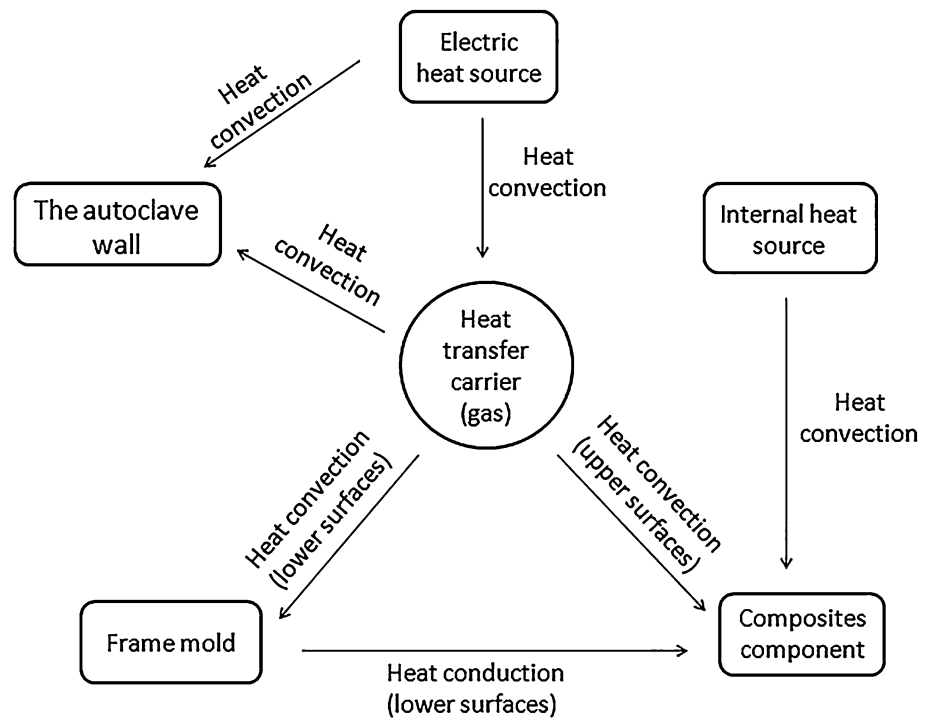
$$Re = \frac{\rho \times u \times L}{\mu}, \tag{1}$$

where L is characteristic length (it represents diameter of autoclaves), u is fluid velocity, ρ is fluid density, and μ is fluid viscosity.

The parameters of air are as follows: room temperature: 298 K, $\rho = 1.24$ kg/m³, $\mu = 17.9e^{-6}$ kg/m s, $u = 2.5$ m/s.

By substituting the above data into the formula (1), the following results are obtained:

$$Re = \frac{\rho \times u \times L}{\mu} = \frac{1.24 \times 2.5 \times 2.5}{17.9e^{-6}} = 432,960 > 12,000.$$

As $Re > 12,000$, the flow state of gas must be a turbulent flow.

Grid generation

When the fluid flows through the mold, the flow velocity will increase rapidly at the micro-space in the normal direction of the molds' surface, until it increases to the same as the inflow velocity. This micro-space is called "boundary layer". Its area is further divided into buffer layer and viscous sublayer. Viscous sublayer is near the solid surface, and the solution of boundary layer mainly focuses on this area. As $Re = 432960$, the turbulence model which has a low value of Re cannot be chosen. However, the turbulence model of high Reynolds number is also not suitable for viscous sublayer. To solve the problem, two methods can be considered. They are the wall function method and the wall model method, respectively. In this study, the grids of boundary layer (as shown in Fig. 7) can directly decide the accuracy of simulation. Therefore, the wall model method is chosen, because it can densify the grids. Considering that the SST turbulence model possesses both the advantages of K-model and K-e model [20], and that the SST model can provide more precise solution of viscous sublayer under the dense grids, therefore, SST model is a suitable choice in this paper. In the grids of boundary layer, the location of grid nodes in the first layer can directly determine the distribution of the entire boundary layer grids, so the distance from the grid nodes of first layer to the wall must be ensured. The distance is defined as "y" in the following contents.

Another value y^+ directly affects the value of y, so the selection of y^+ is very important, and the accuracy of y^+ must be ensured as well. To accurately solve the viscous sublayer, it is necessary to make sure that $y^+ \leq 5$. The following conditions should also be guaranteed: the number of layer is set between 10 and 15, and the height ratio ranges from 1.0 to 1.2. In the computing process of computational fluid dynamics (CFD), the role of y^+ reflects the calculating height of the first boundary layer grid during the process of grid generation [21]. The calculation process is as follows:

(1) Calculating the Reynolds number: Re.
(2) Estimating the wall friction coefficient.
    The calculating formula is defined as:

$$C_f = 0.058 Re^{-0.2}. \tag{2}$$

Fig. 7 Grids in the boundary layer
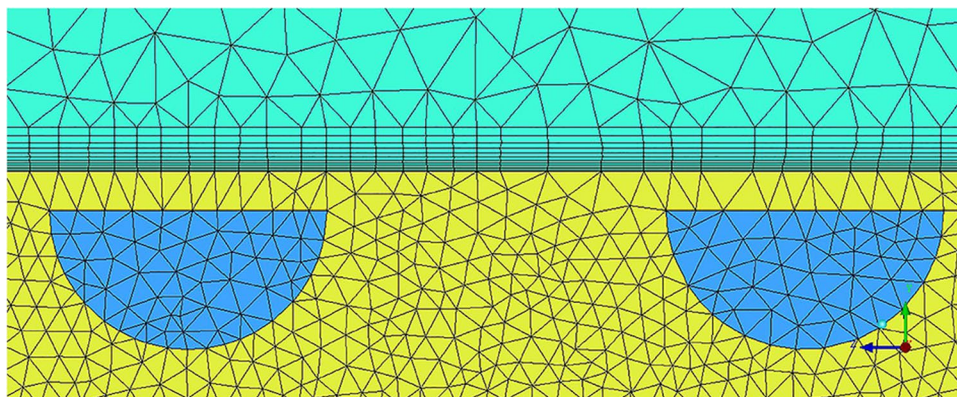
(3) Computing the wall shear stress.
   The calculating formula is defined as:

$$\tau_w = 0.5 C_f \rho u^2, \tag{3}$$

   where u is fluid velocity.

(4) Using the wall shear stress to estimate the speed: u_τ
   The calculating formula is defined as:

$$u_\tau = \sqrt{\frac{\tau_w}{\rho}}. \tag{4}$$

(5) Calculating the grid height of the first layer.

   The calculating formula is defined as:

$$y = \frac{y^+ \mu}{u_\tau \rho}. \tag{5}$$

The value of y^+ can only be obtained through estimation before calculation, because the regional velocity is unknown. When the geometry of calculative area is relatively complex and irregular, we cannot try to make that all the values of y^+ in the wall region become more reasonable, and it will only waste a lot of time and energy. Therefore, the major focus should be taken on the important influential area of the boundary layer. Considering that the geometric structure of frame-type mold is more complicated in the autoclave process, and only the mold's upper surface can contact with composite components, so the upper surface is the main point. To solve the viscous sublayer well, 1 is set as the default for the value of y^+.

The relevant data are taken into the formulas (1–5), and the value of y is 0.2 mm after calculation. The number of boundary layer grids is selected as 12 in this paper, and the growth rate is regarded as 1.2. To limit the grid number of the whole model, the grid size increases gradually from boundary layer region to the fluid region. However, complex geometric shapes need to be ensured to coincide with mesh model at the same time, and the mesh of solid should also increase grids' density. The grids in solid areas can be seen in Fig. 8 [22].
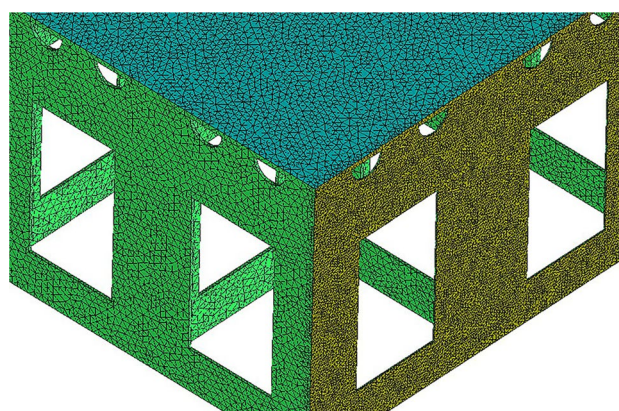

Fig. 8 Grids in solid areas

Mathematical model

Governing equations for convective heat transfer

The processes of flow and heat transfer are distinct as they apply to different occasions, but these processes are dominated by three basic physical laws: mass conservation, momentum conservation, and conservation of energy [23].

Heat transfer in a fluid domain is governed by the following equations [24]:

Mass conservation equation:

$$\frac{\partial \rho}{\partial t} + \text{div}(\rho U) = 0. \tag{6}$$

Momentum conservation equations:

$$\frac{\partial(\rho u)}{\partial t} + \text{div}(\rho u U) = \text{div}(\mu \times \text{grad}(u)) - \frac{\partial p}{\partial x} + S_{Mx}, \tag{7}$$

$$\frac{\partial(\rho v)}{\partial t} + \text{div}(\rho v U) = \text{div}(\mu \times \text{grad}(v)) - \frac{\partial p}{\partial y} + S_{My}, \tag{8}$$

$$\frac{\partial(\rho w)}{\partial t} + \text{div}(\rho w U) = div(\mu \times \text{grad}(w)) - \frac{\partial p}{\partial z} + S_{Mz}. \tag{9}$$

Energy conservation equation:

$$\frac{\partial(\rho h)}{\partial t} + \text{div}(\rho h U) = div(k \times \text{grad}(T)) - p \times \text{div}(U) + \Phi + S_\text{h},$$

(10)

where $\frac{\partial(\rho h)}{\partial t}$ is transient, $\text{div}(\rho h U)$ is convection, $\text{div}(k \times \text{grad}(T))$ is conduction, $p \times \text{div}(U)$ is diffusion, Φ is viscous work, and S_h is sources.

The equation system that is formed by formulas mentioned above cannot be a closed system, so two gas state equations need to be added.

Gas state equations:

$$p = p(\rho, T),$$

(11)

$$h = h(\rho, T),$$

(12)

$U = u \times i + v \times j + w \times k$: component of velocity in the x, y, and z directions.

Here, k is thermal conductivity, T is fluid temperature, p is fluid pressure, λ is the second coefficient of viscosity, S_Mx, S_My, and S_Mz are fluid sources, and S_h is heat source.

Compared with the actual fluid region, the governing equations of the solid zone are relatively simple. There is no flow state in the solid region, so convection and diffusion terms do not exist. Heat conduction is the only way to transfer energy in the solid region.

The boundary conditions of model

Before numerical simulation, model should be simplified, and the corresponding boundary conditions should be set. In this paper, the mold and autoclave are strictly symmetrical body, so the half physical model is used to simulate. The autoclave calculation model is shown in Fig. 9. According to the working principles and actual condition of autoclave, the boundary conditions are set as follows:

1. The surface of autoclave is no-slip and insulating wall.
2. The effective area of the autoclave is an inner cavity with a cylinder space. Its diameter and length are 2.5 and 7 m, respectively. As the influence of fluid flow among inner and external cavity of autoclave on the temperature field is very small, it is no need to take it into consideration.
3. One end of the semi-cylinder is set as the entrance velocity boundary condition. Its speed is 2.5 m/s, and the gas temperature at the inlet is determined by the curing temperature curve. The expression of this curve is: $T = 0.025 \times t + 298$ (K). The other end of semi-cylinder is regarded as outlet and regulated the boundary condition of pressure. Hydrostatic pressure is the default for the pressure.

The mold is set as solid area, and other areas are set as the fluid fields. The simulation lasts 4800 s. The thermocouple is set on the mold's profile before experiment. During the experimental process, the temperature inductor of thermocouple is used to gather temperature data, the paperless recorder is to make temperature data transfer to corresponding value. When the experiment finishes, the temperature change of mold's profile during the entire heating process can be obtained.

Results and discussion

The temperature distribution of mold is shown in Fig. 10. It presents an uneven temperature distribution of mold surface due to the influence of frame type mold's structure. In the mold, the temperature of the windward side is obviously higher than that of the leeward side. This is mainly because the support grids of mold's windward side hinder the move of high temperature airflow, change the flow
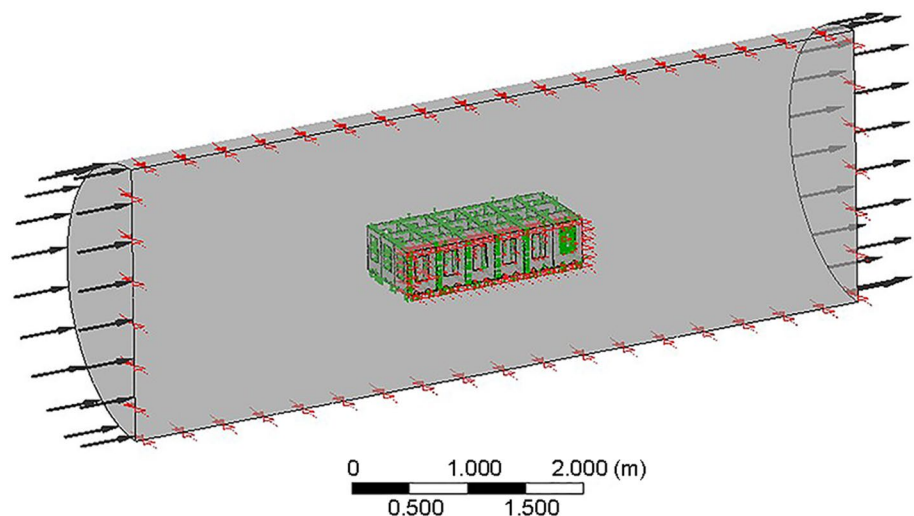
Fig. 9 Autoclave calculation model

0   1.000   2.000 (m)
0.500   1.500

Fig. 10 Temperature distribution of the mold
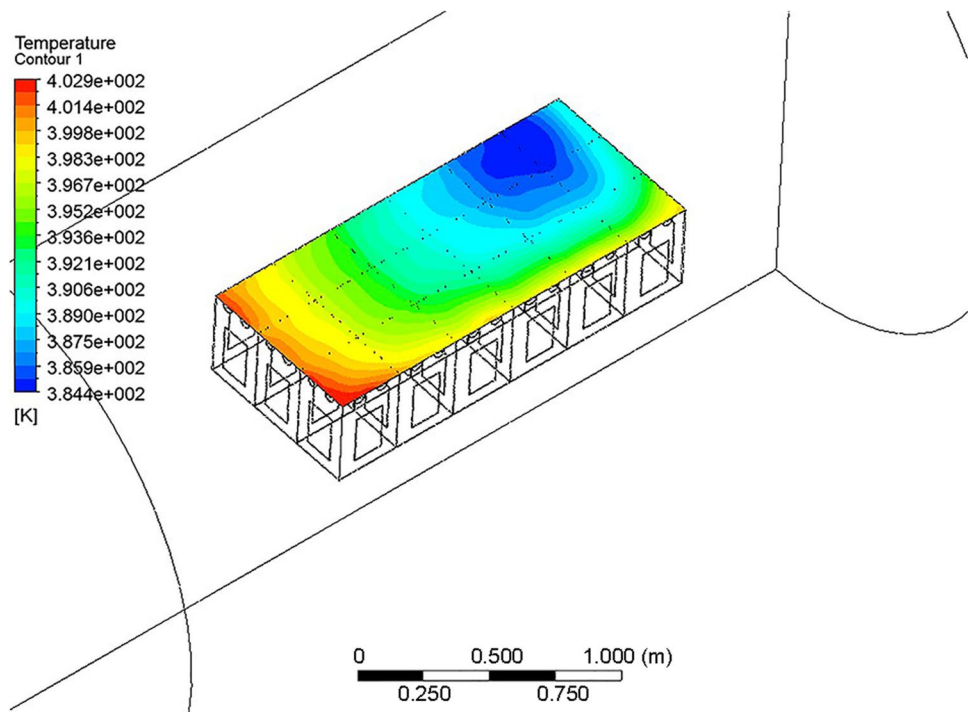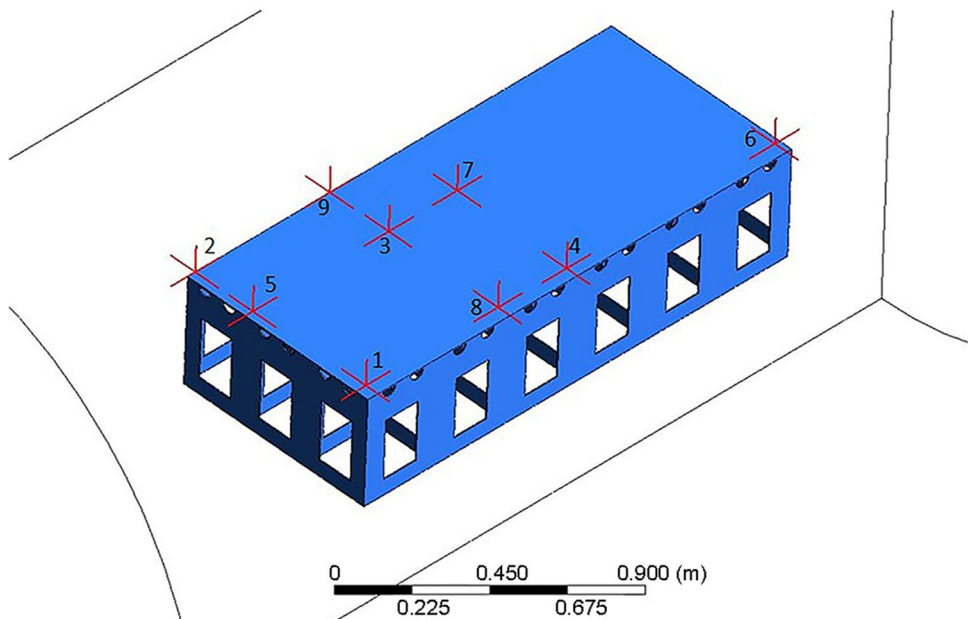

Fig. 11 Monitoring points

direction, and further result in the temperature of mold's leeward side being lower than the windward side. Furthermore, we can see the temperature of the front end, and the side of mold's upper surface is both higher than the inside surface. The reason may be that the convective heat transfer between the molds' periphery and high temperature airflow becomes stronger. The descriptions above are consistent with actual situation.

Some experiment monitoring points are placed to test and verify the data obtained from simulation. Owing to that some monitoring points which do not return data, in nine monitoring points, we choose point 1 to point 6 to validate, as shown in Fig. 11. The results, after comparison, are shown in Fig. 12. As can be seen, at the beginning of heating, the slope of temperature-rising curve is relatively small, and the temperature-rising speed of each point is
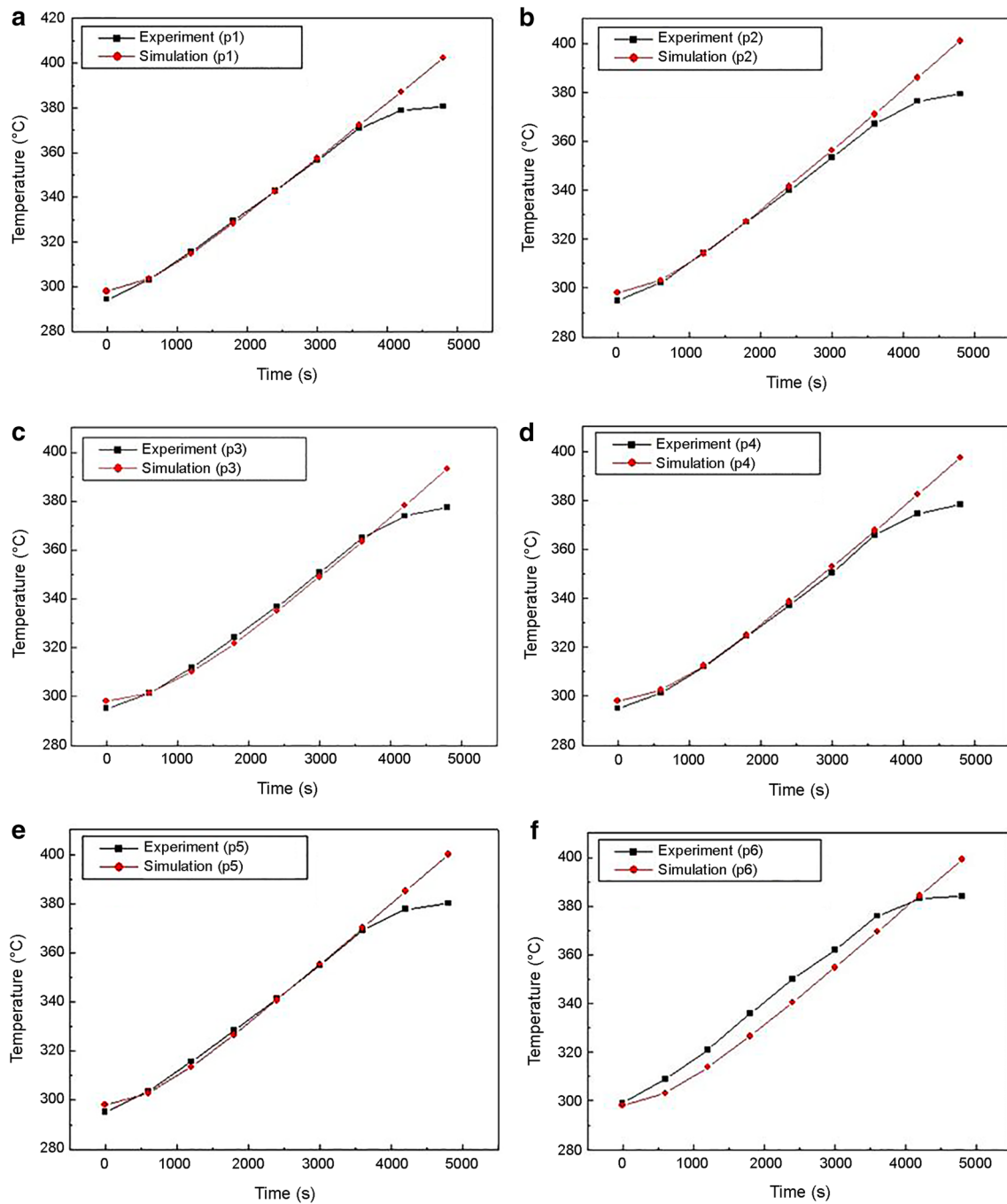
Fig. 12 Comparison between simulation curve and experiment curve

slow. With the increase in heating time, the temperature of point rises faster. Meanwhile, the slope of curve becomes larger. Then, heating rate gradually becomes stable. This is because at the start of heating, the temperature of whole mold is lower than the gas, and the steel as the mold's material is a good conductor for heat transfer. When the heat is conveyed from the high-temperature gas to the surface of mold, the surface will soon transfer the heat to the interior

of mold, and thus, the temperature rises slowly from the start of heating. After heating up for a while, the temperature in the mold has started to rise, and heat-transfer situation of the whole mold tends to be stable. Therefore, the temperature rise curve and its slope tend to be stable.

Overall, the simulated data are in accordance with the experimental data to a great degree, except the data of point 6. At this point, the error is slightly larger. This is because
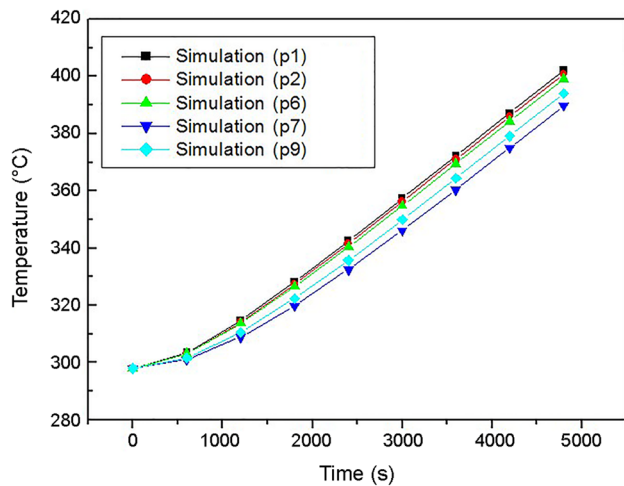
Fig. 13 Comparison between different points

the heat source is at the leeward side of autoclave. That will produce radiative heating on the mold at the leeward side, and it will lead to temperature rise. However, the influence of radiation is neglected before the process of simulation. It further leads to the largest error for point 6. As the maximum error is within 5 % (in the simulation of similar research, accuracy is about 10 %), considering that it satisfies the actual engineering requirement. Therefore, it can be concluded that the simulation data are reliable and the simulation model can be applied to simulate temperature distribution of large frame type mold.

To analyze the temperature rise condition for different positions in the mold surface, five points (1, 2, 6, 7, and 9) are selected, as shown in Fig. 13. The temperature rise curves of the five points comparatively lag behind curing temperature curves. In the entire process of temperature-rising, the temperature of points 1, 2, and 6 is relatively higher. The temperature-rising speeds of these three points are relatively faster and the slowest speed appears at point 7. It indicates that the temperature rise curve of point 7 has the maximum hysteresis. All the above phenomena are caused by the mold structure. As the inhibition of support grids can weaken the effect of heat convection on the middle and leeward sides of the mold, thus, the temperature of point 7 rises slowly.

Conclusion

According to the specific research findings mentioned above, the following conclusions can be drawn.

1. This paper abandons some factors that have little effect on simulation, and mainly focuses on the analysis of boundary layer. To better solve the boundary layer, we

choose to use the SST turbulence model. At the end, the accuracy of simulation on the molds' temperature distribution successfully reaches 5 %.

2. This paper has proved that the boundary layer is actually of great importance to the simulation of molds' temperature distribution in autoclave process. Therefore, the grids of boundary layer must be processed properly to obtain accurate simulation results.

3. This paper has conducted precise simulation on molds' temperature distribution in autoclave process, and verified the simulation results through specific experiment. Research findings indicate that simulation results are in accordance with the actual situation.

References

1. Yan D, Liu W, Huang G (2012) Design study for composites autoclave forming mould. Des Manuf Technol Die Mould 7:49–52
2. Mi Y, Yan Q, Li X, Hong M, Cao M, Zhang X (2015) Effects of temperature induced thermal expansion and oxidation on the Charpy impact property of C/C composites. J Wuhan Univ Technol (Mater Sci Ed) 3:473–477
3. Yue G, Zhang J, Zhang B (2013) Influence of mold on cure-induced deformation of composites structure. Acta Mater Compos Sin 4:206–210
4. Nakhaei MR, Naderi G, Mostafapour A (2016) Effect of processing parameters on morphology and tensile properties of PP/EPDM/organoclay nanocomposites fabricated by friction stir processing. Iran Polym J 25:179–191
5. Gniatczyk JL, Deaver DT (2000) Composite molding tools and processes of forming molding tools. US Patent 6309587 B 1
6. Michael C, Niu Y (2005) Composite airframe structures. Hong Kong Conmilit Press Ltd, Hong Kong
7. Prasad N, Vijay KA, Shishir S (2016) Banana fiber reinforced low-density polyethylene composites: effect of chemical treatment and compatibilizer addition. Iran Polym J 25:229–241
8. Bahramian AR (2013) Effect of external heat flux on the thermal diffusivity and ablation performance of carbon fiber reinforced novolac resin composite. Iran Polym J 22:579–589
9. Duval M (2005) Investigation and modelling of the heat transfer process in carbon fibre/epoxy composite tools. Carleton University, Canada
10. Hudek M (2001) Examination of heat transfer during autoclave processing of polymer composites. MSc Thesis, University of Manitoba, Canada
11. Pirouzfar V, Mosalmani M, Mortezaei M (2015) Experimental study, modeling and optimization to improve heat resistance of modified resole-pitch composites. Iran Polym J 24:829–836
12. Ding J, Huang Y, Han TZ (2016) Functional graphene nanoflakes/cyanate/epoxy nanocomposites: mechanical, dielectric and thermal properties. Iran Polym J 25:69–77
13. Vafayan M, Ghoreishy MHR, Abedini H, Beheshty MH (2015) Development of an optimized thermal cure cycle for a complex-shape composite part using a coupled finite element/genetic algorithm technique. Iran Polym J 24:459–469
14. Gao Y, Qu CH (2012) Numerical simulation about heat-fluid coupling in autoclaves. Ind Furn 4:37–39
15. Zhang X, Gan ZH, Zhang H (2011) Research on optimization of mold temperature fields in autoclave age forming. Manuf Inf Eng China 19:30–37

16. Yue G, Zhang B, Du SH (2010) Influence of the mould on curing induced shape distortion for resin matrix thermosetting composites. Fiber Reinf Plast Compos 5:63–65

17. Zhang CH (2009) Curing temperature field tradeoff design method of large scale composite material structure in autoclave process. Harbin Institute of Technology, Harbin

18. Zhang J (2012) Research on composite molding process in autoclave based on FEA. Nanjing University of Aeronautics and Astronautics, Nanjing

19. Yu G (2011) A technology of temperature field analysis in autoclave processing for airplane composite structures. Nanjing University of Aeronautics and Astronautics, Nanjing

20. Tao W (2009) Numerical heat transfer, 2nd edn. Xi'an Jiaotong University Press, Xi'an

21. Bai G, Yan D, Zhang D (2013) A study on the temperature field distribute property of large frame type molds. Acta Mater Compos Sin 30:169–174

22. Zhang CH, Zhang B, Wang Y (2010) Refined simulation on curing temperature field of composite structures. Dev Appl Mater 3:41–46

23. Zhang CH, Liang X, Wang Y (2011) Rules of impact of autoclave environment on frame mould temperature field of advanced composites. J Mater Sci Eng 4:547–553

24. Han Y, Guo H, Zhang X (2011) Thermal performance analysis of LED with multichips. J Wuhan Univ Technol (Mater Sci Ed) 6:1089–1092